J Appl Physiol 121: 154–163, 2016.
First published May 19, 2016; doi:10.1152/japplphysiol.00832.2015.

Separate and combined effects of a 10-d exposure to hypoxia and inactivity on oxidative function in vivo and mitochondrial respiration ex vivo in humans

Desy Salvadego,[1] Michail E. Keramidas,[2] Lorenza Brocca,[3] Rossana Domenis,[1] Irene Mavelli,[1] Jörn Rittweger,[4,5] Ola Eiken,[2] Igor B. Mekjavic,[6] and Bruno Grassi[1,7]

[1]*Department of Medical and Biological Sciences, University of Udine, Udine, Italy;* [2]*Department of Environmental Physiology, Swedish Aerospace Physiology Centre, Royal Institute of Technology, Stockholm, Sweden;* [3]*Department of Molecular Medicine, University of Pavia, Italy;* [4]*Institute of Aerospace Medicine, German Aerospace Center, Cologne, Germany;* [5]*Children's Hospital, Medical Faculty, University of Cologne, Germany;* [6]*Department of Automation, Biocybernetics and Robotics, Jožef Stefan Institute, Ljubljana, Slovenia; and* [7]*Institute of Bioimaging and Molecular Physiology, National Research Council, Milano, Italy*

Submitted 30 September 2015; accepted in final form 16 May 2016

Salvadego D, Keramidas ME, Brocca L, Domenis R, Mavelli I, Rittweger J, Eiken O, Mekjavic IB, Grassi B. Separate and combined effects of a 10-d exposure to hypoxia and inactivity on oxidative function in vivo and mitochondrial respiration ex vivo in humans. *J Appl Physiol* 121: 154–163, 2016. First published May 19, 2016; doi:10.1152/japplphysiol.00832.2015.—An integrative evaluation of oxidative metabolism was carried out in 9 healthy young men (age, 24.1 ± 1.7 yr mean ± SD) before (CTRL) and after a 10-day horizontal bed rest carried out in normoxia (N-BR) or hypoxia (H-BR, $F_{I_{O_2}}$ = 0.147). H-BR was designed to simulate planetary habitats. Pulmonary O_2 uptake ($\dot{V}O_2$) and vastus lateralis fractional O_2 extraction (changes in deoxygenated hemoglobin+myoglobin concentration, Δ[deoxy(Hb+Mb)] evaluated using near-infrared spectroscopy) were evaluated in normoxia and during an incremental cycle ergometer (CE) and one-leg knee extension (KE) exercise (aimed at reducing cardiovascular constraints to oxidative function). Mitochondrial respiration was evaluated ex vivo by high-resolution respirometry in permeabilized vastus lateralis fibers. During CE $\dot{V}O_{2peak}$ and Δ[deoxy(Hb+Mb)]peak were lower ($P < 0.05$) after both N-BR and H-BR than during CTRL; during KE the variables were lower after N-BR but not after H-BR. During CE the overshoot of Δ[deoxy(Hb+Mb)] during constant work rate exercise was greater in N-BR and H-BR than CTRL, whereas during KE a significant difference vs. CTRL was observed only after N-BR. Maximal mitochondrial respiration determined ex vivo was not affected by either intervention. In N-BR, a significant impairment of oxidative metabolism occurred downstream of central cardiovascular O_2 delivery and upstream of mitochondrial function, possibly at the level of the intramuscular matching between O_2 supply and utilization and peripheral O_2 diffusion. Superposition of hypoxia on bed rest did not aggravate, and partially reversed, the impairment of muscle oxidative function in vivo induced by bed rest. The effects of longer exposures will have to be determined.

muscle inactivity; microgravity; hypoxia; mitochondrial respiration; oxidative function

NEW & NOTEWORTHY

Superposition of 10 days of hypoxia on profound physical inactivity (bed rest) did not aggravate (and partially attenuated) impairment of oxidative function in vivo induced by bed rest alone. The main site(s) of impairment are presumably downstream of cardiovascular function but upstream of mitochondria. The findings add insights into the mechanisms of exercise limitations under environmental stressors such as microgravity/physical inactivity and hypoxic exposure, which characterize Moon and Mars environments as well as different pathological conditions.

PROLONGED INACTIVITY CAN LEAD to extreme degrees of deconditioning in several vital physiological systems and represents a threat for individual health and quality of life. Bed rest (BR) studies are widely used as experimental models to evaluate the physiological consequences of prolonged muscle disuse and unloading (39), a condition commonly experienced by astronauts in microgravity and by individuals exposed to injuries, chronic diseases, and aging. Prolonged periods of BR lead to alterations in oxidative function at several levels from pulmonary function and cardiovascular O_2 delivery to peripheral O_2 utilization (1). In previous 35-day BR studies (44, 47), we have documented a significant impairment of skeletal muscle oxidative metabolism.

Future missions to the Moon or Mars will expose astronauts not only to skeletal muscle inactivity/unloading but also to a substantial hypoxic stimulus (6). Similarly, several important pulmonary, cardiovascular, and metabolic diseases, as well as the aging process, induce a combination of muscle deconditioning by inactivity and cellular hypoxia [see for example (35, 41)]. It is known that chronic H (the effect of which is usually evaluated during and/or after altitude exposure and is commonly associated with a negative energy balance) may impair whole body oxidative function (11, 15); also in this respect, the impairment may be related to pulmonary function, cardiovascular O_2 delivery, and peripheral O_2 utilization (11, 12, 27, 33, 34, 38, 51).

The combined effects of inactivity/unloading and hypoxia on oxidative function have not been systematically studied. When combined, the two stimuli could act synergistically in determining a significant limitation of oxidative metabolism, impairing exercise tolerance, and the quality of life of subjects/astronauts/patients. The aim of the present study is to begin to fill this gap. More specifically, we have used an integrative approach with measurements spanning from whole body O_2 uptake ($\dot{V}O_2$), to skeletal muscle fractional O_2 extraction, to mitochondrial oxidative function ex vivo. Oxidative function was assessed in vivo during incremental cycle ergometer (CE) exercise and dynamic knee extension (KE) exercise with one leg (2). During KE the recruitment of a relatively small muscle mass (i.e., the quadriceps femoris) of one leg removes the

Address for reprint requests and other correspondence: B. Grassi, Dept. of Medical and Biological Sciences, Univ. of Udine, Piazzale M. Kolbe 4, I-33100 Udine, Italy (e-mail: bruno.grassi@uniud.it).

metabolic constraints deriving from central cardiovascular O_2 delivery, thereby allowing a more direct functional assessment of skeletal muscle oxidative performance (2, 45). The intrinsic functional properties of mitochondria were assessed ex vivo in permeabilized muscle fibers obtained by biopsy using high-resolution respirometry (40, 46). The experiments were carried out in healthy young volunteers exposed for 10 days (according to a randomized crossover protocol) to normoxic BR, normobaric hypoxia ($F_{I_{O_2}} = 0.147$, corresponding to an altitude of ~4,000 m), and combined BR and hypoxia. We hypothesized that the superposition of hypoxia on BR (H-BR) would aggravate the impairment of skeletal muscle oxidative function in vivo induced by BR alone (normoxic BR, N-BR). More specifically, we hypothesized that lower peak values of $\dot{V}_{O_2}$ and muscle fractional O_2 extraction during both CE and KE, and a more pronounced impairment of mitochondrial oxidative function ex vivo would be observed after H-BR than after N-BR.

MATERIALS AND METHODS

Subjects

We evaluated nine healthy, recreationally active men whose main physical characteristics at baseline were as follows: age, 24.1 ± 1.7 yr (mean ± SD); body mass (BM), 73.4 ± 12.1 kg; height, 1.79 ± 0.07 m; body mass index (BMI), 22.7 ± 3.1 kg/m^2; and $\dot{V}_{O_{2peak}}$, 43.5 ± 4.7 ml·kg^{-1}·min^{-1}. None of the participants were engaged in competitive sports activities nor did they follow specific training programs before and throughout the study. All participants resided at low altitude (<500 m). Recruitment procedures for participants was based on European Space Agency recommendations (Standardization of bed rest study conditions, version 1.5, August 2009). Exclusion criteria included a medical history of respiratory, hematological, or cardiovascular diseases; altitude exposure (>500 m) in the last 2 mo prior to the experiments; participation in dietary programs during the last 6 mo before the experiments; and use of drugs and/or medications (17). More details on recruitment of subjects can be found in Debevec et al. (17).

Participants were informed about the aims, procedures, and possible risks of the investigation and gave their written informed consent. The study was approved by the National Committee for Medical Ethics at the Ministry of Health of the Republic of Slovenia, and conformed to the Declaration of Helsinki (2000).

Experimental Design and Protocol

The experiments were carried out at the hypoxic facility of the Olympic Sports Centre (Planica-Rateče, Slovenia), which is situated at an altitude of 940 m. The facility has the capability to induce/maintain any simulated altitude on one entire floor comprising 10 double rooms. The simulation of altitude was achieved by reducing O_2 fraction in the rooms/living areas using a Vacuum Pressure Swing Adsorption system (b-Cat, Tiel, The Netherlands). The ambient fraction of oxygen was continuously monitored and adjusted to the target simulated altitude [see (36)].

Each participant underwent three 10-day campaigns in a randomized order: normobaric normoxic (fraction of inspired O_2, $F_{I_{O_2}} = 0.209$; $P_{I_{O_2}} = 133.3 \pm 0.2$ mmHg) horizontal bed rest (N-BR); normobaric hypoxic ($F_{I_{O_2}} = 0.144$; $P_{I_{O_2}} = 91.6 \pm 0.1$ mmHg, target simulated altitude of ~4,000 m) horizontal bed rest (H-BR); and normobaric hypoxic ($F_{I_{O_2}} = 0.144$; $P_{I_{O_2}} = 91.6 \pm 0.1$ mmHg) ambulatory confinement (H-AMB). The interventions were separated by 4-wk washout periods to allow the effects of prior exposure to hypoxia and/or bed rest to be eliminated.

The ascent to the target simulated altitude in the H-BR and H-AMB trials was achieved over a 3-day period (*day 1*, 3,000 m; *day 2*, 3,400 m; *day 3* and thereafter, 4,000 m) in agreement with the recommendations of the International Mountain Medicine Society.

During the bed rest interventions (N-BR and H-BR), no deviations from the lying position, nor muscle stretching or static contractions were permitted. Subjects in the H-AMB condition were allowed to move freely within the hypoxic area and were engaged in two 30-min bouts of aerobic exercise per day (stepping at a rate of 100 steps/min on a 30-cm step). Adherence to the assigned protocol was ensured using continuous closed-circuit television surveillance and constant supervision by researchers and medical staff. Details on study design and physical activity and daily energy intakes during interventions are reported in Debevec et al. (17). Other research groups carried out measurements of pulmonary, cardiovascular, metabolic, hematologic, immunologic, and other functions [as described in (17)]. Measurements included in this study were performed over 4 days before (CTRL), and over 2 days after each intervention. CE exercises were carried out the day before KE exercises. The environmental conditions within the facility remained stable throughout the experimental sessions (ambient temperature, 22.4 ± 2.1°C; relative humidity, 40 ± 11%; and ambient pressure, 689 ± 6 mmHg). All tests were conducted under close medical supervision and following standard safety procedures.

Before data collection, subjects were allowed time to gain familiarity with the investigators and experimental setup, and were familiarized with the exercise protocols by means of short, preliminary practice runs. Incremental exercise protocols were carried out by using a electromagnetically braked cycle ergometer (Daum Electronic, Furth, Germany) and a custom-built knee extension ergometer [modified Monark cycle ergometer, see (47)] as originally described by Andersen et al. (2).

During CE, subjects performed an initial 2-min of pedaling at 60 W, thereafter 25-W increments were imposed every minute until the limit of tolerance. Pedaling frequency was digitally displayed to the subjects, who were asked to keep a constant cadence throughout the tests of between 65 and 70 revolutions per minute.

During KE subjects were constrained on an adjustable seat by a safety belt, which anchored the angle of the hip at ~90°. Subjects pushed on a padded bar attached to a lever arm connected to the crank of the cycle ergometer, and allowing a knee extension between ~90 to ~170°. This type of exercise confines muscle contractile activity to the quadriceps femoris muscle of one leg, which is activated during the extension phase. The return of the leg to the starting position is brought about passively by the momentum of the flywheel of the ergometer [see (47) for details]. After an initial 2 min of unloaded KE exercise, an incremental test was performed with the right leg. Work rate was increased by 6 W every minute to allow the subjects to reach the limit of tolerance in ~10 min. Work rate was applied by adjusting the tension of a strap around the ergometer flywheel, as in a mechanically braked cycle ergometer. Throughout the test the active KE and passive knee flexion cycle was carried out ~40 times per minute as imposed by a metronome. During each cycle (total duration 1.5 s) KE lasted ~1 s. In other words, muscle contraction corresponded to ~65% of the duty cycle.

All exercises were conducted up to the limit of tolerance, which was defined as the inability to maintain the imposed work rate at the required frequency and through the full range of motion despite vigorous encouragement by the operators. Mean values of ventilatory, pulmonary gas exchange, heart rate variables, and muscle oxygenation indices (see below) were calculated during the last 30 s of each work rate; values obtained during the exhausting work rate were considered peak values.

Measurements

Anthropometry. BM and regional and whole body composition were assessed before and immediately after each campaign with dual-energy X-ray absorptiometry (DEXA) using a fan-beam densi-

tometer (Discovery W QDR series; Hologic, Bedford, MA). More details on the DEXA technique and analysis are reported in Debevec et al. (17). The lean mass of the lower limbs was measured as the sum of the fat-free masses of the legs and thighs. Skinfold measurements were made by a caliper at the site of the near-infrared spectroscopy (NIRS) probe on the vastus lateralis muscle to estimate skin and subcutaneous adipose tissue thickness.

Measurements during the incremental tests. Pulmonary ventilation ($\dot{V}_E$), tidal volume (Vt), respiratory frequency (fR), O_2 uptake ($\dot{V}_{O_2}$), and CO_2 output ($\dot{V}_{CO_2}$) were determined on a breath-by-breath basis by means of a metabolic unit (Quark CPET; Cosmed, Italy). Expiratory flow measurements were performed by a turbine flow meter calibrated before each experiment by a 3-liter syringe at three different flow rates. Calibration of O_2 and CO_2 analyzers was performed before each experiment by using gas mixtures of known composition. The gas-exchange ratio (R) was calculated as $\dot{V}_{CO_2}/\dot{V}_{O_2}$. During CE $\dot{V}_{O_2}$ and $\dot{V}_{O_{2peak}}$, values were expressed as m/min and were normalized per unit of BM and lower limbs lean mass ($ml \cdot min^{-1} \cdot kg^{-1}$); during KE, $\dot{V}_{O_{2peak}}$ values were expressed as ml/min and normalized for the lean mass of the thigh.

Heart rate was determined by ECG. Arterial blood O_2 saturation (SaO_2) was continuously monitored by pulse oximetry ($MicrO_2$; Siemens Medical Systems, Danvers, MA) at the finger. Ratings of perceived exertion for dyspnea and limb effort were obtained at rest and at every work rate of the incremental exercise using the Borg modified CR10 scale (7). Peak power output was taken as index of performance.

Blood analyses. Blood samples were drawn from the antecubital vein before and after each intervention. Blood sample collection and analyses are described by McDonnell et al. (36). Blood volume and hemoglobin mass were not determined.

Skeletal muscle oxygenation. Local muscle oxygenation profiles of the vastus lateralis muscle during exercise were evaluated by NIRS. Principles, limitations, and potential applications of this method have been discussed in detail in other reviews (9, 19). NIRS measurements in muscle tissue have been shown to be well correlated with local venous O_2 saturation (9, 52, 54). A limitation of the NIRS approach is related to the fact that only a relatively small and superficial (28) portion of the muscle can be investigated.

A portable near-infrared continuous-wave instrument (PortaMon; Artinis, The Netherlands) was used in this study. Specific details on the method can be found in recent papers by our group (46, 47). The instrument measures micromolar changes in oxygenated hemoglobin (Hb) + myoglobin (Mb) concentrations (Δ[oxy(Hb+Mb)]), and in deoxygenated [Hb + Mb] (Δ[deoxy(Hb+Mb)]) with respect to an initial value arbitrarily set equal to zero and obtained during the resting condition preceding the test. The sum of the two variables (Δ[total(Hb+Mb)]) is related to changes in the total Hb volume in the muscle region of interest.

In contracting muscle, Δ[deoxy(Hb+Mb)] is relatively insensitive to changes in blood volume and has been considered an estimate of skeletal muscle fractional O_2 extraction [ratio between O_2 consumption ($\dot{V}_{O_2}$) and O_2 delivery ($\dot{Q}_{O_2}$)] (20, 23, 30). A physiological calibration of Δ[deoxy(Hb+Mb)] values was performed by obtaining a transient ischemia of the limb after the exercise period (44): data obtained during exercise were expressed as a percentage of the values of maximal muscle deoxygenation obtained by pressure cuff inflation (at 300-350 mmHg) carried out at the inguinal crease of the thigh for a few minutes until Δ[deoxy(Hb+Mb)] increase reached a plateau.

The presence of a deoxygenation overshoot (transitory sharp increase in Δ[deoxy(Hb+Mb)] above the steady-state level occurring after exercise onset) was investigated during the first 2 min of constant work rate CE and KE by performing a two-exponential fitting [see (44)]. The amplitude of the overshoot was measured as the difference between the peak and the steady-state Δ[deoxy(Hb+Mb)] value. The area under the Δ[deoxy(Hb+Mb)] overshoot was calculated by integrating values between the measured response and the steady-state value from the onset of the response until the time at which the steady state was first attained (3). This variable is correlated with the dynamics of muscle O_2 delivery vs. muscle $\dot{V}_{O_2}$: the greater the area under the Δ[deoxy(Hb+Mb)] overshoot the slower the dynamics of muscle O_2 delivery relative to that of muscle $\dot{V}_{O_2}$ (3). The overall area under the curve of the Δ[deoxy(Hb+Mb)] vs. time response was also calculated from the onset until the end of the constant work rate exercise.

Skeletal muscle biopsy and high-resolution respirometry. Muscle samples were obtained from the vastus lateralis muscle of the left limb by percutaneous biopsy, which was taken in all subjects 1 day before the first intervention and on the last day of each intervention. Biopsies were taken at the same time of the day after an overnight fast. The subjects refrained from strenuous exercise up to 24 h prior to the biopsy. The biopsy was obtained after anesthesia of the skin; the subcutaneous fat tissue and the muscle fascia with 2–4 ml of 2% lidocaine hydrochloride (xylocain). A small incision was then made to penetrate skin and fascia, and the muscle sample was harvested using a Bergstrom biopsy needle (5).

The muscle samples were divided into two portions. One portion (~20 mg wet weight) was immediately frozen in liquid nitrogen and stored at −80°C until determination of citrate synthase (CS) protein expression. The other portion (~15 mg wet weight) was used to evaluate mitochondrial respiration ex vivo (40), and was immediately placed in an ice-cold preservation solution (BIOPS; Oroboros Instruments, Innsbruck, Austria) containing EGTA-calcium buffer (10 mM) (free Ca^{2+} concentration 100 nmol/l), imidazole (20 mM), taurine (20 mM), K^+/4 morpholinoethanesulfonic acid (50 mM), dithiothreitol (0.5 mM), $MgCl_2$ (6.56 mM), ATP (5.77 mM), and phosphocreatine (15 mM), pH 7.1.

Fiber bundles were separated with sharp-ended needles, leaving only small areas of contact incubated in the above solution (4°C) containing 10% (wt/vol) fatty acid-free BSA and 30% (vol/vol) DMSO, and snap-frozen in liquid nitrogen. The samples were stored at −80°C until analysis, which was carried out within 1 mo [for details see (46, 55)].

For analysis, the fiber bundles were quickly thawed in a water bath at 37°C and washed in BIOPS containing 2 mg/ml BSA to remove any residual DMSO from the tissue. Fibers were then incubated in 5 ml of BIOPS (4°C) containing 50 g/ml saponin for 30 min with continuous gentle stirring to ensure complete permeabilization. After being rinsed twice for 10 min in a respiration medium (MiR05; Oroboros Instruments: 0.5 mM EGTA, 60 mM potassium lactobionate, 3 mM $MgCl_2 \cdot 6H_2O$, 20 mM taurine, 10 mM KH_2PO_4, 20 mM HEPES, 110 mM sucrose, and 1 g/l BSA, pH 7.1), permeabilized fibers were measured for wet weight and immediately transferred into a respirometer (Oxygraph-2k; Oroboros Instruments) for analysis.

Mitochondrial respiratory function was evaluated by measuring O_2 consumption polarographically by high-resolution respirometry (40). Data were digitally recorded using DatLab4 software (Oroboros Instruments). The instrumentation allows for O_2 consumption measurements with small amounts of sample in closed respiration chambers containing 3 ml of air-saturated respiration medium at 37°C; 3–5 mg of muscle fibers was used for the analysis. Standardized instrumental and chemical calibrations were performed to correct for back-diffusion of O_2 into the chamber from the various components, leak from the exterior, O_2 consumption by the chemical medium, and by the sensor O_2 (40). The O_2 concentration in the chamber was maintained between 300 and 400 μM (average O_2 partial pressure ~250 mmHg) to avoid O_2 limitation of respiration. Intermittent reoxygenation steps were performed during the experiments by adding a 200 mM hydrogen peroxide solution into the medium containing catalase (40). All respirometric analyses were carried out in duplicate.

A substrate-uncoupler-inhibitor-titration protocol with a substrate combination that matches physiological intracellular conditions was applied (40). Nonphosphorylating resting mitochondrial respiration was measured in the presence of malate (4 mM) and glutamate

(10 mM), and in the absence of adenylates so that O_2 consumption was mainly driven by the back leakage of protons through the inner mitochondrial membrane ("leak" respiration). ADP-stimulated mitochondrial respiration sustained by complex I (*state 3* respiration) was measured by stepwise additions of ADP (2.5 mM) as phosphate acceptor, with malate and glutamate as substrates. Succinate (10 mM) was added to support convergent electron flow into the Q-junction through complexes I and II. Maximal ADP-stimulated mitochondrial respiration was then determined in the presence of saturating [ADP] (5 mM). The addition of cytochrome *c* (10 μM) had no significant additive effects on respiration, with minor increases of approximately 5–7%, thereby confirming the integrity of the outer mitochondrial membrane. We also examined electron transport system capacity by stepwise addition of the chemical uncoupler protonophore carbonyl-cyanide-p-trifluoromethoxyphenylhydrazone (FCCP) to optimum concentration (1.25 μM). Rotenone (1 μM) and antimycin A (2.5 μM) were added to inhibit complexes I and III, providing a measure of residual O_2 consumption, indicative of nonmitochondrial O_2 consumption. Mitochondrial respiration was then corrected for O_2 flux due to the residual O_2 consumption. The degree of coupling of oxidative phosphorylation for a specific substrate supply (glutamate and malate in this case) was determined by calculating the ratio between *state 3* respiration minus leak respiration and *state 3* respiration [(*state 3* − leak)/*state* 3] (see 22).

Western blotting. Frozen muscle samples were pulverized and resuspended in a lysis buffer [20 mM Tris·HCl, 1% Triton X-100, 10% glycerol, 150 mM NaCl, 5 mM EDTA, 100 mM NaF, and 2 mM NaPPi supplemented with protease and phosphatase inhibitors (Sigma-Aldrich) and 1 mM PMSF]. The homogenate obtained was centrifuged at 18,000 *g* for 20 min at 4°C. Muscle-extracted proteins (15 μg) were loaded on gradient precast gels (AnyKd; Bio-Rad, Hercules, CA) and were electro-transferred to nitrocellulose membranes at 100 V for 2 h at 4°C. The membranes were incubated with the anti-CS primary antibodies (Abcam, Cambridge, MA) overnight. Thereafter, the membranes were blocked in 5% milk and then incubated in anti-rabbit IgG horseradish peroxidase-conjugated secondary antibody (Cell Signaling) for 1 h. The protein bands were visualized by an enhanced chemiluminescence method. The content of CS protein was assessed by determining the brightness-area product of the protein band and normalizing on actin content, as previously described (10).

Statistical Analysis

Results are expressed as means ± standard deviations (SD). To evaluate the effects of N-BR and H-BR, linear mixed effect (LME) models were constructed with subject as random effect and H-AMB data excluded. For gas exchange and muscle oxygenation variables, time (Before vs. After), condition (N-BR vs. H-BR), and their interaction were used as fixed effects. Data from the baseline collection phases were lumped together. For data of mitochondrial respiration and CS expression, because there was only one common baseline muscle biopsy, the fixed effects were coded as TimeCondition with levels Before, After N-BR, and After H-BR. The H-AMB data were then analyzed via LME with time as random effect and subject as fixed effect. LME models were optimized according to Akaike's information criterion. Data were box-cox transformed when nonlinear quantile-quantile plots or heteroscedasticity were found. Models for statistical testing of the primary hypothesis were simplified in a step-wise manner. First, the time∗condition interaction term was discarded when justified by nonsignificance and Akaike's criterion, and the condition term was discarded in the next step. Any significant effects were followed up with treatment contrasts using baseline and N-BR as reference. Data fitting by exponential functions was performed using the least squares residuals method. Comparisons between fittings with different exponential models were carried out using the *F*-test.

Level of significance was set at 0.05. Statistical analyses were carried out with software packages (GraphPad Prism 5.0, GraphPad Software, SPSS 13.0.1).

RESULTS

Values for BM, BMI, lean body mass (LBM), lean mass of the lower limbs and thigh, and fat body mass are reported in Table 1. BM and LBM decreased by 3–4% after all interventions. The lean mass of lower limbs and thighs decreased significantly (by ~5%) after H-BR, whereas it remained substantially unchanged after N-BR and H-AMB. Fat body mass did not change after the interventions. Skin and adipose tissue thickness, measured at the site of placement of the NIRS probe, ranged between 6.5 and 19.5 mm (11.5 ± 4.2), and was not altered by any of the interventions.

Blood [Hb] before the BR studies (CTRL) was 154.6 ± 8.4 g/l. It increased by ~4% after N-BR (160.1 ± 8.1) and by ~12% after H-BR (173.9 ± 6.5) and H-AMB (173.7 ± 12.0). All changes were statistically significant; values obtained after H-BR and H-AMB were significantly higher than those obtained after N-BR. [Hb] values before each intervention were not different.

Peak values of the main cardiovascular, ventilatory, and gas-exchange variables determined at exhaustion are presented in Tables 2 (CE) and 3 (KE). Peak HR values during KE were in all conditions ~35% lower than those obtained during CE; this confirms that the peak work rate in KE, although being maximal for the type of exercise, did not represent a maximal burden for the cardiovascular system.

Both during CE and KE, $\dot{V}O_{2\,peak}$ (ml/min) (Fig. 1) and vastus lateralis Δ[deoxy(Hb+Mb)] peak (% of the values obtained during a transient limb ischemia) (Fig. 2) were lower during N-BR than CTRL. During H-BR, on the other hand, $\dot{V}O_{2peak}$ and Δ[deoxy(Hb+Mb)] peak values were lower only during CE, and not during KE. No differences were observed

Table 1. *Anthropometric and body composition characteristics of subjects*

	CTRL	N-BR	H-BR	H-AMB
Body mass, kg	73.4 ± 12.1	72.4 ± 12.7	71.1 ± 11.9*	72.0 ± 11.2
Body mass index, kg/m^2	22.7 ± 3.0	22.3 ± 2.9	21.9 ± 2.9*	22.3 ± 2.6
Lean body mass, kg	56.1 ± 6.3	54.3 ± 6.0*	53.6 ± 6.7*	53.9 ± 6.1*
Lean lower limb mass, kg	17.7 ± 2.2	17.4 ± 2.6	16.8 ± 2.4*†	17.1 ± 2.2
Lean thigh mass, kg	6.4 ± 0.9	6.3 ± 1.0	6.1 ± 0.9*	6.2 ± 0.8
Fat body mass, kg	17.3 ± 6.2	18.1 ± 6.8	17.5 ± 6.0	18.2 ± 5.8
ATT (mm)	11.5 ± 4.2	11.6 ± 2.9	11.2 ± 3.8	11.4 ± 4.8

Data are expressed as means ± SD. CTRL, control condition; N-BR, normoxic bed rest; H-BR, hypoxic bed rest; H-AMB, hypoxic ambulatory confinement. ATT, skin and subcutaneous adipose tissue thickness at the site of placement of the near-infrared spectroscopy probe. *Significantly different vs. CTRL ($P < 0.05$). †Significantly different vs. N-BR ($P < 0.05$).

Table 2. *Peak values of the main investigated variables determined at the limit of tolerance during incremental cycle ergometer exercise*

	CTRL	N-BR	H-BR	H-AMB
Power output$_{peak}$, W	286 ± 44	273 ± 49*	267 ± 52*	290 ± 45
$\dot{V}E_{peak}$, l/min	136.5 ± 19.2	136.2 ± 22.7	136.8 ± 20.2	147.5 ± 23.7*
VT$_{peak}$, liter	2.72 ± 0.33	2.65 ± 0.24	2.70 ± 0.28	2.69 ± 0.29
fR$_{peak}$, breaths/min	51.0 ± 8.8	52.0 ± 9.6	51.3 ± 8.9	55.6 ± 11.5
$\dot{V}O_{2peak}$, l/min	3.23 ± 0.47	2.98 ± 0.50*	3.00 ± 0.54*	3.19 ± 0.60
$\dot{V}O_{2peak}$/BM, ml·kg^{-1}·min^{-1}	43.5 ± 4.7	40.8 ± 4.6*	41.4 ± 4.7	43.3 ± 4.0
$\dot{V}O_{2peak}$/two-leg mass, ml·kg^{-1}·min^{-1}	183.1 ± 17.6	171.4 ± 17.1*	179.6 ± 22.1	186.5 ± 19.6
$\dot{V}O_{2peak}$, l/min	3.91 ± 0.52	3.59 ± 0.58*	3.49 ± 0.64*	3.70 ± 0.51
R$_{peak}$	1.22 ± 0.07	1.21 ± 0.07	1.16 ± 0.05*	1.18 ± 0.06
$PET_{O_{2peak}}$, mmHg	105.1 ± 3.5	108.0 ± 3.6	107.5 ± 3.7	107.9 ± 5.4
$PET_{CO_{2peak}}$, mmHg	33.5 ± 3.2	30.8 ± 3.5	29.2 ± 4.0	29.7 ± 4.9
HR$_{peak}$, beats/min	188 ± 5	190 ± 7	189 ± 7	190 ± 7
SaO_2, %	93.8 ± 1.9	93.7 ± 3.0	94.2 ± 1.3	93.3 ± 2.2
RPE-dyspnea scores, 0–10	9.2 ± 1.6	9.3 ± 1.7	9.3 ± 2.0	9.6 ± 0.8
RPE-leg effort scores, 0–10	9.2 ± 1.2	8.3 ± 1.9	8.3 ± 2.1	9.0 ± 2.0
Δ[oxy(Hb+Mb)]$_{peak}$, μM	−7.3 ± 2.4	−4.4 ± 1.9*	−4.7 ± 3.5*	−6.2 ± 3.7
Δ[deoxy(Hb+Mb)]$_{peak}$, μM	14.4 ± 4.2	11.8 ± 4.2*	12.1 ± 3.7*	13.6 ± 4.6
Δ[tot(Hb+Mb)]$_{peak}$, μM	7.1 ± 4.6	7.4 ± 5.4	7.3 ± 5.4	7.4 ± 6.2

Data are means ± SD. $\dot{V}E$, pulmonary ventilation; VT, tidal volume; fR, respiratory frequency; $\dot{V}O_2$, O_2 uptake; BM, body mass; $\dot{V}CO_2$ CO_2 output; R, gas exchange ratio; PET_{O_2}, O_2 end-tidal pressure; PET_{CO_2}, CO_2 end-tidal pressure; HR, heart rate; SaO_2, arterial blood O_2 saturation; RPE, ratings of perceived exertion. Near-infrared spectroscopy-derived micromolar changes in oxygenated hemoglobin+myoglobin concentrations, Δ[oxy(Hb+Mb)]; deoxygenated Hb+Mb concentrations, Δ[deoxy(Hb+Mb)]; oxygenated+deoxygenated Hb+Mb concentrations, Δ[total(Hb+Mb)]. *Significantly different from CTRL ($P < 0.05$).

between H-AMB and CTRL for either variable or type of exercise. When $\dot{V}O_{2\,peak}$ was expressed per unit of body mass or was normalized for the lean mass of the lower limbs (CE) or for the lean mass of the thigh (KE), values were still significantly lower after N-BR but not after H-BR (Tables 2 and 3).

Vastus lateralis muscle oxygenation indices obtained by NIRS at exhaustion during CE and KE, expressed as micromolar changes with respect to a resting value arbitrarily set equal to zero (see MATERIALS AND METHODS) are also reported in Tables 2 and 3. Peak changes in local muscle blood volume during exercise, as estimated by Δtotal(Hb+Mb)] peak, were not affected by any intervention, during either CE or KE.

Figure 3 shows typical individual profiles of Δ[deoxy-(Hb+Mb)] dynamics during the first 2 min of CE (constant work rate at 60 W) and unloaded KE. These analyses were performed for eight of nine subjects; one subject was excluded because of a low signal-to-noise ratio. In a typical subject shown in Figure 3, no substantial overshoot of Δ[deoxy-(Hb+Mb)] (see MATERIALS AND METHODS) was observed in CTRL or H-AMB, during both CE and KE; after N-BR a clear overshoot was observed during CE and KE; the overshoot was present but less pronounced after H-BR.

The mean (± SD) values of the amplitude of the overshoot, the area under the overshoot, and the area under the overall Δ[deoxy(Hb+Mb)] response are reported in Table 4. Whereas the amplitude of the overshoot and the area under the overshoot were higher after N-BR compared with the other experimental conditions, no significant differences were described for the

Table 3. *Peak values of the main investigated variables determined at the limit of tolerance during incremental knee-extension exercise*

	CTRL	N-BR	H-BR	H-AMB
Power output$_{peak}$, W	58 ± 7	61 ± 7	58 ± 12	57 ± 6
$\dot{V}E_{peak}$, l/min	42.8 ± 8.5	42.2 ± 9.3	45.3 ± 8.1	44.1 ± 7.7
VT$_{peak}$, liter	1.45 ± 0.32	1.48 ± 0.43	1.50 ± 0.48	1.52 ± 0.40
fR$_{peak}$, breaths/min	29.9 ± 7.3	28.5 ± 6.9	30.1 ± 6.7	29.3 ± 7.2
$\dot{V}O_{2peak}$, l/min	0.91 ± 0.07	0.84 ± 0.08*	0.86 ± 0.07	0.89 ± 0.06
$\dot{V}O_{2peak}$/BM, ml·kg^{-1}·min^{-1}	12.6 ± 1.6	11.8 ± 1.6*	12.3 ± 1.7	12.5 ± 1.5
$\dot{V}O_{2peak}$/TM, ml·kg^{-1}·min^{-1}	143.1 ± 14.9	134.7 ± 16.2*	143.1 ± 15.6	144.4 ± 12.6
$\dot{V}CO_{2peak}$, l/min	1.06 ± 0.06	0.99 ± 0.07*	1.01 ± 0.08	1.03 ± 0.06
R$_{peak}$	1.16 ± 0.12	1.18 ± 0.14	1.18 ± 0.16	1.16 ± 0.11
$PET_{O_{2peak}}$, mmHg	101.7 ± 3.4	102.8 ± 4.5	104.6 ± 4.2	103.6 ± 2.7
$PET_{CO_{2peak}}$, mmHg	34.5 ± 2.0	33.7 ± 2.4	32.0 ± 2.6	32.2 ± 1.9
HR$_{peak}$, breaths/min	120 ± 12	130 ± 16	128 ± 19	122 ± 14
SaO_2, %	98.8 ± 0.5	98.6 ± 1.3	98.2 ± 0.8	98.7 ± 1.2
RPE-dyspnea scores, 0–10	2.0 ± 1.0	2.4 ± 1.3	2.3 ± 0.8	2.0 ± 1.1
RPE-leg effort scores, 0–10	9.4 ± 0.8	9.7 ± 0.7	9.7 ± 0.5	9.7 ± 1.0
Δ[oxy(Hb+Mb)]$_{peak}$, μM	−7.2 ± 3.4	−4.0 ± 2.7*	−5.3 ± 4.5	−5.8 ± 3.4
Δ[deoxy(Hb+Mb)]$_{peak}$, μM	14.3 ± 5.9	12.1 ± 5.1*	13.3 ± 6.0	13.9 ± 5.3
Δ[tot(Hb+Mb)]$_{peak}$, μM	7.3 ± 6.2	8.0 ± 5.8	8.0 ± 5.9	8.1 ± 7.5

Data are means ± SD. TM, thigh mass; R, pulmonary gas-exchange ratio, RPE, ratings of perceived exertion. *Significantly different from CTRL ($P < 0.05$).

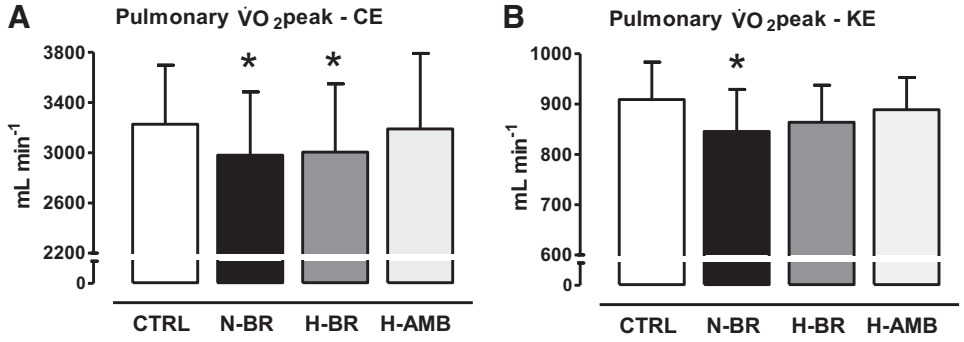

Fig. 1. Mean (± SD) values of pulmonary $\dot{V}O_{2\ peak}$ (ml/min) obtained during cycle ergometer (CE) (*A*) and knee extension (KE) (*B*) exercises in control conditions (CTRL) and after normoxic bed rest (N-BR), hypoxic bed rest (H-BR), and ambulatory confinement (H-AMB). *$P < 0.05$ vs. CTRL.

area under the overall response. These observations applied to both CE and KE.

The main data related to mitochondrial respiration determined ex vivo in isolated permeabilized fibers are presented in Figure 4. Maximal ADP-stimulated mitochondrial respiration was not significantly affected by any intervention. The maximal capacity of the electron transport system induced by the chemical uncoupler FCCP was also not significantly affected by any intervention. Mitochondrial leak respiration was not affected by N-BR, whereas it increased after H-BR (by ~10%) and after H-AMB (by ~20%), reaching statistical significance in the latter experimental condition. The degree of coupling of oxidative phosphorylation [(*state 3* − leak)/*state 3*] at a specific substrate supply (glutamate and malate) did not change after N-BR, whereas it decreased significantly after H-BR and H-AMB. Expression of CS, taken as an estimate of mitochondrial content, was not significantly different among the experimental conditions (2.97 ± 0.54 arbitrary units in CTRL, 2.63 ± 0.37 in N-BR, 2.82 ± 0.39 in H-BR, and 2.69 ± 0.61 in H-AMB).

DISCUSSION

Measurements in the present study were carried out in normoxia on healthy young men before and after 10 days of exposure to N-BR, H-AMB (FI_{O_2} = 0.144), and H-BR. The study yielded two main results.

First, refuting our hypothesis, superposition of hypoxia on BR did not aggravate the BR-induced impairment of peak oxidative performance in vivo, as evaluated by peak $\dot{V}O_2$, peak skeletal muscle fractional O_2 extraction, and profiles of O_2 extraction during constant work rate exercise. This occurred both during CE and one-leg KE exercise in which central cardiovascular constraints are removed or significantly attenuated. For some of the investigated variables, superposition of hypoxia on BR attenuated the impairments observed after BR alone, possibly as a consequence, at least in part, of enhanced muscle O_2 delivery/peripheral O_2 diffusion attributable to the increased [Hb].

Second, refuting our hypothesis, superposition of hypoxia on BR did not affect mitochondrial maximal respiratory function ex vivo, which was maintained after all experimental exposures.

Thus substantial impairments to the oxidative function in vivo were observed downstream of cardiovascular O_2 delivery (as demonstrated by the results during KE) but upstream of mitochondria (as demonstrated by the results of high-resolution respirometry), thus at the level of the intramuscular matching between O_2 delivery and O_2 utilization (as suggested by the O_2 extraction profiles during constant work rate exercise) and/or of peripheral O_2 diffusion, and were mainly determined by inactivity-unloading.

These findings relate to relatively short (10 days) experimental exposures. No inferences can be made regarding longer periods or chronic exposures. It cannot be excluded that with longer exposures to hypoxia oxidative function could be affected in vivo, and that the superposition of hypoxia on BR could aggravate the impairment induced by the two separate stimuli. Nor can it be excluded that longer exposures would impair mitochondrial function ex vivo.

Exposure to hypoxia by itself (H-AMB) did not induce changes in any of the investigated variables. Although hypoxia negatively affected some variables of mitochondrial respiratory function (leak respiration, coupling of oxidative phosphorylation), these impairments were presumably not substantial enough to affect the oxidative function in vivo. Or, alternatively, any metabolic impairment deriving from hypoxia was overcome by an enhanced O_2 delivery deriving from the hypoxia-driven increased [Hb]. In the present study we did not

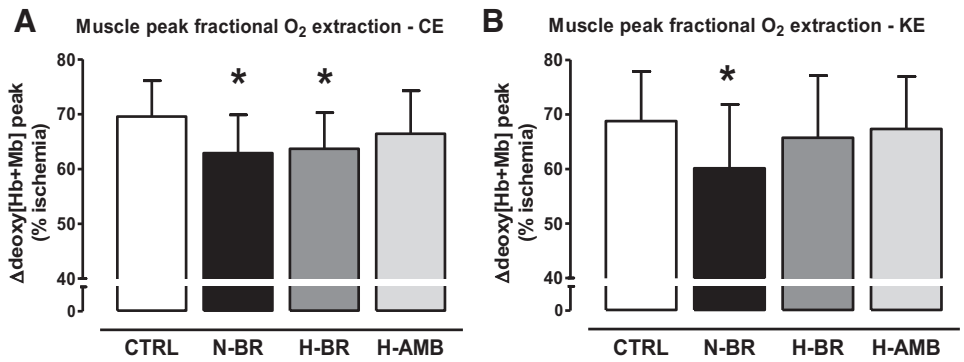

Fig. 2. Mean (± SD) values of peak vastus lateralis muscle deoxygenation (Δ[deoxy-(Hb+Mb)]) obtained using near-infrared spectroscopy, which estimates peak fractional O_2 extraction during CE (*A*) and KE (*B*) exercises. Δ[deoxy(Hb+Mb)] data are expressed as a percentage of values obtained during a transient limb ischemia at the end of the test. *$P < 0.05$ vs. CTRL.

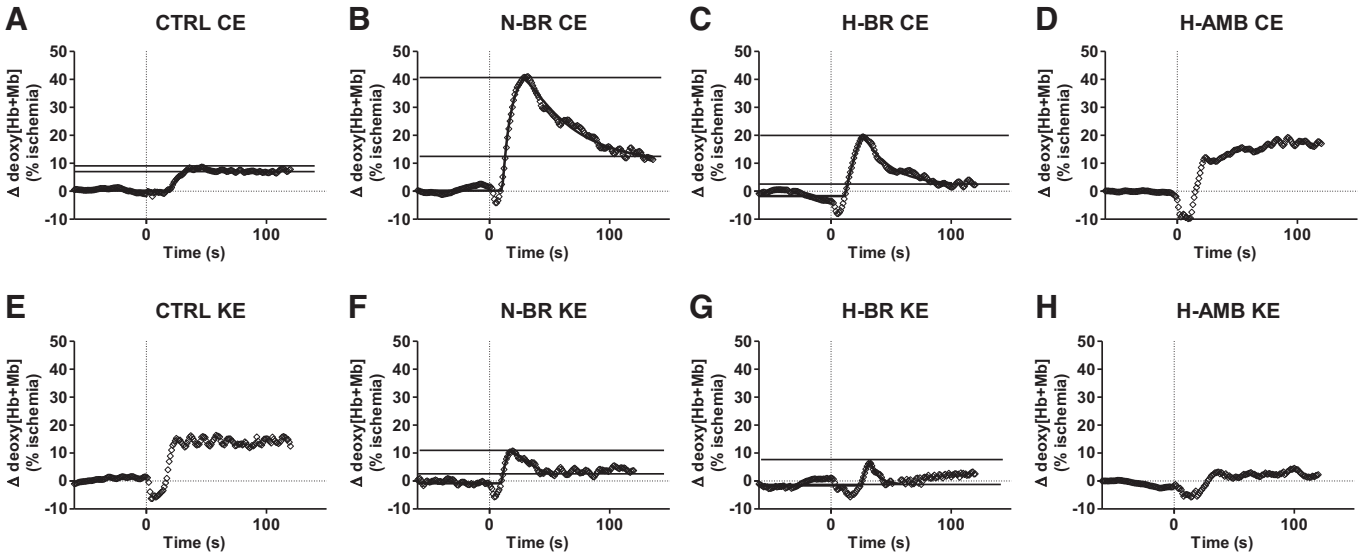

Fig. 3. Typical examples of the dynamics of Δ[deoxy(Hb+Mb)] during the first 2 min of CE and KE (constant work rate cycling at 60 W and unloaded KE) during CTRL, and after N-BR, H-BR, and H-AMB (subject 3). The presence of a transient deoxygenation overshoot was checked by fitting the responses with a two-component equation (solid line). The amplitude of the overshoot is indicated by the horizontal solid lines.

determine Hb mass or blood volume. Although an increased erythropoiesis represents a classical finding after hypoxia exposure, it cannot be excluded that the increased blood [Hb] values observed in the present study following H-BR could be determined, at least in part, by a decreased blood volume, which is known to occur both during BR (39) and hypoxia (53). It should be pointed out, however, that an increased [Hb] could by itself induce an enhanced O_2 delivery by enhancing peripheral O_2 diffusion (18).

The hypothesis of a protective effect represented by the hypoxia-induced increased [Hb] may also appear to be in contradiction with the observation of unchanged microvascular Hb content as estimated by the Δ[total(Hb+Mb)] determined by NIRS. Although a dissociation between changes in macrovascular and microvascular hematocrit has been described before by Sarelius et al. (48), it should be remembered that Δ[total(Hb+Mb)] determined by NIRS needs to be considered with some caution because this variable, differently from Δ[oxy(Hb+Mb)] and Δ[deoxy(Hb+Mb)], cannot undergo the physiological calibration by the transient ischemia (see MATERIALS AND METHODS).

We used Δ[deoxy(Hb+Mb)] to estimate fractional O_2 extraction, which reflects the unbalance between the intramuscular increases in $\dot{V}O_2$ and O_2 delivery (20, 23, 30). Interesting observations were made in the present study in relation to the time course of Δ[deoxy(Hb+Mb)] during constant work rate exercise (the initial period of the incremental test). The overall degree of mismatch between O_2 delivery and $\dot{V}O_2$ (see the area under the Δ[deoxy(Hb+Mb)] vs. time curve) was not significantly different among conditions either during CE or KE. Nonetheless, after N-BR and (to a lesser extent) after H-BR a transient overshoot of Δ[deoxy(Hb+Mb)] occurring during the first ~60 s (range 43–120 s) of exercise was observed both during CE and (albeit less pronounced) during KE; no overshoot was observed at CTRL or after H-AMB.

This overshoot is considered to be caused by a sluggish intramuscular O_2 delivery with respect to $\dot{V}O_2$ (14, 21, 25, 41) and would be conceptually similar to the transient undershoot of microvascular PO_2 as estimated by phosphorescence quenching [see for example (4, 41)]. The transient mismatch could derive from a suboptimal nitric oxide signaling within the muscle, which would uncouple the heterogeneous microvascular blood flow

Table 4. *Muscle deoxygenation overshoot during the first minutes of CE and KE exercises*

	CTRL	N-BR	H-BR	H-AMB
Cycle ergometer				
Amplitude Δ[deoxy(Hb+Mb)] overshoot, % ischemia	2.3 ± 3.2	11.5 ± 5.7*	6.6 ± 8.0	0.3 ± 0.9
Area under Δ[deoxy(Hb+Mb)] overshoot, %·s	37.2 ± 53.6	264.6 ± 179.4*	154.2 ± 193.8	4.7 ± 13.4
Area under Δ[deoxy(Hb+Mb)] response, %·s	1171 ± 324	782 ± 322	900 ± 261	1191 ± 344
Δ[deoxy(Hb+Mb)] overshoot, % total response	8.1 ± 11.7	35.5 ± 16.1*	17.4 ± 19.8	0.5 ± 1.5
Knee extension				
Amplitude Δ[deoxy(Hb+Mb)] overshoot, % ischemia	0.4 ± 0.9	5.1 ± 2.8*†	3.1 ± 3.5	0.9 ± 2.5
Area under Δ[deoxy(Hb+Mb)] overshoot, %·s	3.5 ± 9.9	62.4 ± 45.6*†	37.8 ± 45.6	7.4 ± 21.0
Area under Δ[deoxy(Hb+Mb)] response, %·s	935 ± 287	645 ± 465	930 ± 359	1153 ± 664
Δ[deoxy(Hb+Mb)] overshoot, % total response	0.5 ± 1.4	15.2 ± 12.4*†	6.2 ± 7.4	0.4 ± 1.0

Data are means ± SD. Amplitude and area under muscle deoxygenation (Δ[deoxy(Hb+Mb)]) overshoot (expressed in % of the maximal muscle deoxygenation during transient limb ischemia) were measured during the first 2 min of constant work rate, cycle ergometer (CE) and knee extension. The "overshoot component" was calculated as the area of the deoxygenation overshoot relative to the overall area of the Δ[deoxy(Hb+Mb)] response. *Significantly different from CTRL. †Significantly different from CE ($P < 0.05$).

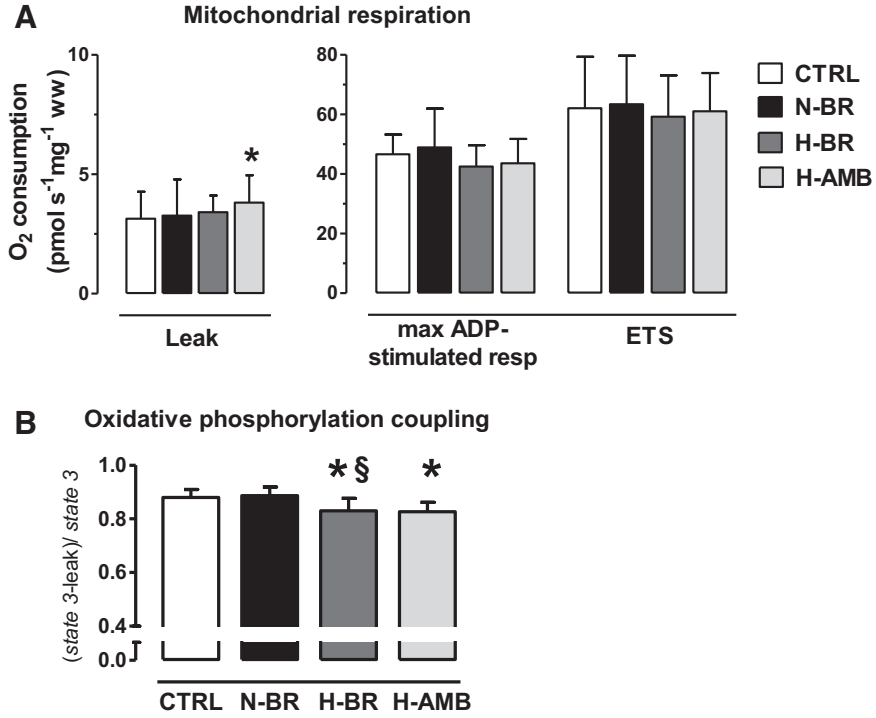

Fig. 4. *A*: variables in mitochondrial respiratory function expressed per unit of tissue mass (wet weight) measured in permeabilized muscle fibers. Leak: resting respiratory rate in the presence of glutamate and malate without ADP (*left* axis). Maximal ADP-stimulated mitochondrial respiration determined with 5 mM ADP and glutamate, malate, and succinate as substrates (*right* axis). ETS, maximal capacity of the electron transport system induced by carbonylcyanide-p-trifluoromethoxyphenylhydrazone (FCCP) (*right* axis). *B*: oxidative phosphorylation coupling [(*state 3* − leak)/*state 3*], variable estimating the degree of coupling of oxidative phosphorylation. Values are presented as means (± SD). *$P <$ 0.05 vs. CTRL. §$P < 0.05$ vs. N-BR.

increase from the presumably heterogeneous O_2 uptake (25, 29, 41). The Δ[deoxy(Hb+Mb)] overshoot would determine a decreased microvascular PO_2, and thereby a decreased driving pressure for peripheral O_2 diffusion and an impaired oxidative metabolism during the initial, critical part of the metabolic transition (42). An overshoot in Δ[deoxy(Hb+Mb)] during metabolic transitions has been described in subjects exposed to 35 days of BR (44) and, among others, in patients with chronic obstructive pulmonary disease (16), chronic heart failure (49), or metabolic myopathies (43). Also for this variable, hypoxia attenuated the impairment attributable to BR alone.

In the present study mitochondrial oxidative function was evaluated ex vivo by high-resolution respirometry on permeabilized skeletal muscle fibers as an attempt to determine whether changes in these variables could in part explain changes in oxidative function observed in vivo. Measurements were carried out in acute conditions of unlimited O_2 availability. Although in healthy, physically active individuals and in physiological conditions muscle mitochondrial oxidative capacity exceeds maximal O_2 delivery to the working muscles (8), previous studies carried out on sedentary subjects (24) or young individuals exposed to prolonged BR (10) highlighted the key role of mitochondrial dysfunction in determining muscle deconditioning after long-term inactivity-unloading.

Maximal ADP-stimulated respiration and maximal electron flow throughout the mitochondrial respiratory chain were not significantly altered after any of the experimental conditions. Ten days of N-BR did not impair mitochondrial respiration ex vivo; the scenario could be different following longer BR periods [see the proteomic data in (10)]. After H-AMB and H-BR nonsignificant trends toward a lower maximal ADP-stimulated respiration (vs. CTRL and N-BR) were observed. These data confirm those obtained by the Lundby group of researchers (26) after subacute (9–11 days) exposure to 4,559 m, and support the hypothesis made by the same authors about a trend toward a progressive decrease in muscle mitochondrial oxidative capacity during prolonged hypoxic exposures (26, 27). The novel finding of the present study was that the superposition of hypoxia on BR for 10 days did not alter maximal mitochondrial O_2 utilization ex vivo.

Mitochondrial content of the tissue from the muscle biopsy as estimated by the expression of CS was not affected by any intervention. In terms of hypoxia, the finding appears to be in agreement with previous investigations (33) showing that the mitochondrial pool and biogenesis were still maintained after subacute hypoxia. Also for this variable, the superposition of hypoxia on BR for 10 days did not determine a mitochondrial loss per unit of muscle mass. In the presence of a slight decrease in muscle mass (see above), however, an unchanged mitochondrial content in the investigated sample would be associated with a slightly decreased mitochondrial mass.

Higher leak respiration and a lower degree of coupling of oxidative phosphorylation were described following hypoxia (associated or not with BR). A lower coupling efficiency indicates that a smaller portion of the mitochondrial membrane potential is linked to ATP synthesis, whereas a greater portion is wasted through proton leak/slip across the inner membrane. The finding is consistent with an upregulation of muscle protein UCP-3, a putative mediator of proton leakage, following subacute hypoxic exposure (33) and would represent a protective mechanism for cells against an excessive mitochondrial reactive oxygen species formation, albeit at the cost of a reduced ATP production.

Limitations. In the present study, high-resolution respirometry measurements could not be carried out immediately after the experimental exposures, but were performed in the laboratory on frozen and subsequently thawed muscle samples (see MATERIALS AND METHODS). Conflicting results on the possibility

of freezing and thawing the samples undergoing high-resolution respirometry are present in the literature. According to Kuznetsov et al. (31) cryopreservation of samples, according to a specific protocol, for up to 1 mo does not significantly alter respirometry measurements. The protocol proposed by Kuznetsov et al. (31) was used in the present study because it was carried out in previous studies by Wüst et al. (55), Cannavino et al. (13), and Tam et al. (50). On the other hand, according to Larsen et al. (32) and Meyer et al. (37), cryopreservation of samples can result in an underestimation of maximal ADP-stimulated mitochondrial respiration (37). However, the same authors observed an excellent correlation ($r^2 = 0.82$) between respirometry measurements in fresh and cryopreserved samples. Moreover, in the studies that raised doubts about the possibility of cryopreserving the samples, significant damage to the outer mitochondrial membrane was likely present, as suggested by the substantial increase in mitochondrial respiration following administration (in the measurement chamber) of cytochrome *c* (32, 37). To stimulate mitochondrial respiration, the administered cytochrome *c* has to reach the mitochondrial matrix, which is impossible in the presence of an intact mitochondrial membrane. In the present study [as well as in the studies by Wüst et al. (55), Cannavino et al. (13), and Tam et al. 50)] the increase in mitochondrial respiration following administration of cytochrome *c* was very small (approximately 5–7%), well within the limits allowing the exclusion of significant damage of the outer mitochondrial membrane. It cannot be excluded, however, that the freeze-thaw procedure used in the present study led to some underestimation of maximal ADP-stimulated mitochondrial respiration.

Conclusions. Ten days of exposure to inactivity resulted in impaired skeletal muscle oxidative metabolism in vivo but it did not affect mitochondrial respiration ex vivo. Substantial impairments to oxidative function in vivo were observed downstream of central cardiovascular O_2 delivery (see the data obtained during KE) but upstream of mitochondrial function (see the high-resolution respirometry data), which is at the level of the intramuscular matching between O_2 delivery and O_2 uptake and/or peripheral O_2 diffusion. Superposition of hypoxia on inactivity did not aggravate the impairment of oxidative function in vivo, but attenuated or prevented some of its manifestations, possibly as a consequence of the enhanced muscle O_2 delivery/peripheral O_2 diffusion from the increased [Hb]. The effects of longer exposures will have to be determined. The results should be of interest to those seeking a better understanding of the physiological adaptations to planetary habitats (environments characterized by both microgravity and hypoxia), as well as the pathophysiology of conditions characterized by the association of inadequate O_2 delivery and physical inactivity.

ACKNOWLEDGMENTS

We thank the staff of the LunHab 2011 project: Dr. A. McDonnell (Jožef Stefan Institute, Ljubljana) for coordination in loco of the project, all the assistants for their excellent technical collaboration and supervision of the subjects during the experimental campaigns, and the subjects who enthusiastically participated in this study. Special thanks to M. Vrhovec (Jožef Stefan Institute, Ljubljana) and to R. Burelli for technical assistance, and to Prof. M. Isola for the help with statistical analyses.

GRANTS

Financial support was provided by the European Space Agency Programme for European Cooperating States Contract 4000104372/11/NL/KML, by Slovene Research Agency Contract L3-3654, and by the EU VII Framework Programme (PlanHab project Grant 284438).

DISCLOSURES

No conflicts of interest, financial or otherwise, are declared by the authors.

AUTHOR CONTRIBUTIONS

D.S., O.E., I.B.M., and B.G. conception and design of research; D.S., M.E.K., L.B., and R.D. performed experiments; D.S., M.E.K., L.B., R.D., and J.R. analyzed data; D.S., I.M., O.E., I.B.M., and B.G. interpreted results of experiments; D.S. prepared figures; D.S. drafted manuscript; D.S., I.M., J.R., and B.G. edited and revised manuscript; D.S., M.E.K., L.B., R.D., I.M., J.R., O.E., I.B.M., and B.G. approved final version of manuscript.

REFERENCES

1. **Ade CJ, Broxterman RM, Barstow TJ.** $\dot{V}O_{2max}$ and microgravity exposure: convective versus diffusive O_2 transport. *Med Sci Sports Exerc* 47: 1351–1361, 2015.
2. **Andersen P, Adams RP, Sjøgaard G, Thorboe A, Saltin B.** Dynamic knee extension as model for study of isolated exercising muscle in humans. *J Appl Physiol* 59: 1647–1653, 1985.
3. **Barbosa PB, Bravo DM, Neder JA, Ferreira LF.** Kinetics analysis of muscle arterial-venous O_2 difference profile during exercise. *Respir Physiol Neurobiol* 173: 51–57, 2010.
4. **Behnke BJ, Delp MD, Dougherty PJ, Musch TI, Poole DC.** Effects of aging on microvascular oxygen pressures in rat skeletal muscle. *Respir Physiol Neurobiol* 146: 259–268, 2005.
5. **Bergström J.** Muscle electrolytes in man. *Scand J Clin Lab Invest Suppl.* 68, 1–110, 1962.
6. **Bodkin DK, Escalera P, Bocam KJ.** A human lunar surface base and infrastructure solution. In: *Space 2006, SPACE Conferences and Exposition*. Reston, VA: American Institute of Aeronautics and Astronautics, 2006. doi: 10.2514/6.2006–7336.
7. **Borg G.** *Borg's perceived exertion and pain scales*. Champaign, IL: Human Kinetics, 1998.
8. **Boushel R, Gnaiger E, Calbet JA, Gonzalez-Alonso J, Wright-Paradis C, Sondergaard H, Ara I, Helge JW, Saltin B.** Muscle mitochondrial capacity exceeds maximal oxygen delivery in humans. *Mitochondrion* 11: 303–307, 2011.
9. **Boushel R, Langberg H, Olesen J, Gonzales-Alonzo J, Bülow J, Kjaer M.** Monitoring tissue oxygen availability with near infrared spectroscopy (NIRS) in health and disease. *Scand J Med Sci Sports* 11: 213–222, 2001.
10. **Brocca L, Cannavino J, Coletto L, Biolo G, Sandri M, Bottinelli R, Pellegrino MA.** The time course of the adaptations of human muscle proteome to bed rest and the underlying mechanisms. *J Physiol* 590: 5211–5230, 2012.
11. **Calbet JA, Boushel R, Rådegran G, Søndergaard H, Wagner PD, Saltin B.** Why is $\dot{V}O_{2\,max}$ after altitude acclimatization still reduced despite normalization of arterial O_2 content? *Am J Physiol Regul Integr Comp Physiol* 284: R304–R316, 2003.
12. **Calbet JA, Rådegran G, Boushel R, Saltin B.** On the mechanisms that limit oxygen uptake during exercise in acute and chronic hypoxia: role of muscle mass. *J Physiol* 587: 477–490, 2009.
13. **Cannavino J, Brocca L, Sandri M, Grassi B, Bottinelli R, Pellegrino MA.** The role of alterations in mitochondrial dynamics and PGC-1α over-expression in fast muscle atrophy following hindlimb unloading. *J Physiol* 593: 1981–1995, 2015.
14. **Casey DP, Joyner MJ.** Local control of skeletal muscle blood flow during exercise: influence of available oxygen. *J Appl Physiol* 111: 1527–1538, 2011.
15. **Cerretelli P, Hoppeler H.** Morphologic, and metabolic response to chronic hypoxia: the muscle system. In: *Handbook of Physiology, Section 4, Vol. 4, Environmental Physiology*. Edited by Fregly MJ, Blatteis CM. New York: Oxford University Press, 1996, pp. 1155–1181.
16. **Chiappa GR, Borghi-Silva A, Ferreira LF, Carrascosa C, Oliveira CC, Maia J, Gimenes AC, Queiroga F Jr, Berton D, Ferreira EM, Nery LE, Neder JA.** Kinetics of muscle deoxygenation are accelerated at the onset of heavy-intensity exercise in patients with COPD: relationship to central cardiovascular dynamics. *J Appl Physiol* 104: 1341–1350, 2008.
17. **Debevec T, McDonnell AC, Macdonald IA, Eiken O, Mekjavic IB.** Whole body and regional body composition changes following 10-day

hypoxic confinement and unloading-inactivity. *Appl Physiol Nutr Metab* 39: 386–395, 2014.
18. **Federspiel WJ, Popel AS.** A theoretical analysis of the effect of the particulate nature of blood on oxygen release in capillaries. *Microvasc Res* 32: 164–189, 1986.
19. **Ferrari M, Muthalib M, Quaresima V.** The use of near infrared spectroscopy in understanding skeletal muscle physiology: recent developments. *Philos Trans A Math Phys Eng Sci* 369: 4577–4590, 2011.
20. **Ferreira LF, Koga S, Barstow TJ.** Dynamics of noninvasively estimated microvascular O_2 extraction during ramp exercise. *J Appl Physiol* 103: 1999–2004, 2007.
21. **Ferreira LF, Poole DC, Barstow TJ.** Muscle blood flow-O_2 uptake interaction and their relation to on-exercise dynamics of O_2 exchange. *Respir Physiol Neurobiol* 147: 91–103, 2005.
22. **Gnaiger E.** *Cell ergometry: OXPHOS and ETS coupling efficiency. Mitochondr Physiol Network 19.13*. Innsbruck, Austria: OROBOROS MiPNet Publications, 2014.
23. **Grassi B.** Delayed metabolic activation of oxidative phosphorylation in skeletal muscle at exercise onset. *Med Sci Sports Exerc* 37: 1567–1573, 2005.
24. **Haseler LJ, Lin AP, Richardson RS.** Skeletal muscle oxidative metabolism in sedentary humans: ^{31}P-MRS assessment of O_2 supply and demand limitations. *J Appl Physiol* 97: 1077–1081, 2004.
25. **Heinonen I, Koga S, Kalliokoski KK, Musch TI, Poole DC.** Heterogeneity of muscle blood flow and metabolism: influence of exercise, aging, and disease states. *Exerc Sport Sci Rev* 43: 117–124, 2015.
26. **Jacobs RA, Boushel R, Wright-Paradis C, Calbet JA, Robach P, Gnaiger E, Lundby C.** Mitochondrial function in human skeletal muscle following high-altitude exposure. *Exp Physiol* 98: 245–255, 2013.
27. **Jacobs RA, Siebenmann C, Hug M, Toigo M, Meinild AK, Lundby C.** Twenty-eight days at 3454-m altitude diminishes respiratory capacity but enhances efficiency in human skeletal muscle mitochondria. *FASEB J* 26: 5192–5200, 2012.
28. **Koga S, Barstow TJ, Okushima D, Rossiter HB, Kondo N, Ohmae E, Poole DC.** Validation of a high-power, time-resolved, near-infrared spectroscopy system for measurement of deep and superficial muscle deoxygenation during exercise. *J Appl Physiol* 118: 1435–1442, 2015.
29. **Koga S, Rossiter HB, Heinonen I, Musch TI, Poole DC.** Dynamic heterogeneity of exercising muscle blood flow and O_2 utilization. *Med Sci Sports Exerc* 46: 860–876, 2014.
30. **Kowalchuk JM, Rossiter HB, Ward SA, Whipp BJ.** The effect of resistive breathing on leg muscle oxygenation using near-infrared spectroscopy during exercise in men. *Exp Physiol* 87: 601–611, 2002.
31. **Kuznetsov AV, Kunz WS, Saks V, Usson Y, Mazat JP, Letellier T, Gellerich FN, Margreiter R.** Cryopreservation of mitochondria, and mitochondrial function in cardiac and skeletal muscle fibers. *Anal Biochem* 319: 296–303, 2003.
32. **Larsen S, Wright-Paradis C, Gnaiger E, Helge JW, Boushel R.** Cryopreservation of human skeletal muscle impairs mitochondrial function. *Cryo Letters* 33: 170–176, 2012.
33. **Levett DZ, Radford EJ, Menassa DA, Graber EF, Morash AJ, Hoppeler H, Clarke K, Martin DS, Ferguson-Smith AC, Montgomery HE, Grocott MP, Murray AJ; Caudwell Xtreme Everest Research Group.** Acclimatization of skeletal muscle mitochondria to high-altitude hypoxia during an ascent of Everest. *FASEB J* 26: 1431–1441, 2012.
34. **Lundby C, Calbet JA, Robach P.** The response of human skeletal muscle tissue to hypoxia. *Cell Mol Life Sci* 66: 3615–3623, 2009.
35. **Maltais F, Decramer M, Casaburi R, Barreiro E, Burelle Y, Debigaré R, Dekhuijzen PN, Franssen F, Gayan-Ramirez G, Gea J, Gosker HR, Gosselink R, Hayot M, Hussain SN, Janssens W, Polkey MI, Roca J, Saey D, Schols AM, Spruit MA, Steiner M, Taivassalo T, Troosters T, Vogiatzis I, Wagner PD; ATS/ERS Ad Hoc Committee on Limb Muscle Dysfunction in COPD.** An official American Thoracic Society/European Respiratory Society statement: update on limb muscle dysfunction in chronic obstructive pulmonary disease. *Am J Respir Crit Care Med* 189: e15–e62, 2014.
36. **McDonnell AC, Eiken O, Mekjavic PJ, Mekjavic IB.** Circadian rhythm of peripheral perfusion during 10-day hypoxic confinement and bed rest. *Eur J Appl Physiol* 11: 2093–2104, 2014.
37. **Meyer A, Charles AL, Zoll J, Guillot M, Lejay A, Singh F, Schlagowski AI, Isner-Horobeti ME, Pistea C, Charloux A, Geny B.** Cryopreservation with dimethyl sulfoxide prevents accurate analysis of skinned skeletal muscle fibers mitochondrial respiration. *Biochimie* 100: 227–233, 2014.
38. **Murray AJ, Horscroft JA.** Mitochondrial function at extreme high altitude. *J Physiol* 594: 1137–1149, 2016.
39. **Pavy-Le Traon A, Heer M, Narici MV, Rittweger J, Vernikos J.** From space to Earth: advances in human physiology from 20 years of bed rest studies (1986–2006). *Eur J Appl Physiol* 101: 143–194, 2007.
40. **Pesta D, Gnaiger E.** High-resolution respirometry. OXPHOS protocols for human cell cultures and permeabilized fibers from small biopsies of human muscle. *Methods Mol Biol* 810: 25–58, 2012.
41. **Poole DC, Hirai DM, Copp SW, Musch TI.** Muscle oxygen transport and utilization in heart failure: implications for exercise (in)tolerance. *Am J Physiol Heart Circ Physiol* 302: H1050–H1063, 2012.
42. **Poole DC, Jones AM.** Oxygen uptake kinetics. *Compr Physiol* 2: 933–996, 2012.
43. **Porcelli S, Marzorati M, Belletti M, Bellistri G, Morandi L, Grassi B.** The "second wind" in McArdle's disease patients during a second bout of constant work rate submaximal exercise. *J Appl Physiol* 116: 1230–1237, 2014.
44. **Porcelli S, Marzorati M, Lanfranconi F, Vago P, Pišot R, Grassi B.** Role of skeletal muscles impairment and brain oxygenation in limiting oxidative metabolism during exercise after bed rest. *J Appl Physiol* 109: 101–111, 2010.
45. **Richardson RS, Poole DC, Knight DR, Kurdak SS, Hogan MC, Grassi B, Johnson EC, Kendrick KF, Erickson BK, Wagner PD.** High muscle blood flow in man: is maximal O_2 extraction compromised? *J Appl Physiol* 75: 1911–1916, 1993.
46. **Salvadego D, Domenis R, Lazzer S, Porcelli S, Rittweger J, Rizzo G, Mavelli I, Simunic B, Pisot R, Grassi B.** Skeletal muscle oxidative function in vivo and ex vivo in athletes with marked hypertrophy from resistance training. *J Appl Physiol* 114: 1527–1535, 2013.
47. **Salvadego D, Lazzer S, Marzorati M, Porcelli S, Rejc E, Simunic B, Pisot R, di Prampero PE, Grassi B.** Functional impairment of skeletal muscle oxidative metabolism during knee extension exercise after bed rest. *J Appl Physiol* 111: 1719–1726, 2011.
48. **Sarelius IH.** Microcirculation in striated muscle after acute reduction in systemic hematocrit. *Respir Physiol* 78: 7–17, 1989.
49. **Sperandio PA, Borghi-Silva A, Barroco A, Nery LE, Almeida DR, Neder JA.** Microvascular oxygen delivery-to-utilization mismatch at the onset of heavy-intensity exercise in optimally treated patients with CHF. *Am J Physiol Heart Circ Physiol* 297: H1720–H1728, 2009.
50. **Tam E, Bruseghini P, Calabria E, Sacco LD, Doria C, Grassi B, Pietrangelo T, Pogliaghi S, Reggiani C, Salvadego D, Schena F, Toniolo L, Verratti V, Vernillo G, Capelli C.** Gokyo Khumbu/Ama Dablam Trek 2012: effects of physical training and high-altitude exposure on oxidative metabolism, muscle composition, and metabolic cost of walking in women. *Eur J Appl Physiol* 116: 129–144, 2016.
51. **Viganò A, Ripamonti M, De Palma S, Capitanio D, Vasso M, Wait R, Lundby C, Cerretelli P, Gelfi C.** Proteins modulation in human skeletal muscle in the early phase of adaptation to hypobaric hypoxia. *Proteomics* 8: 4668–4679, 2008.
52. **Vogiatzis I, Habazettl H, Louvaris Z, Andrianopoulos V, Wagner H, Zakynthinos S, Wagner PD.** A method for assessing heterogeneity of blood flow and metabolism in exercising normal human muscle by near-infrared spectroscopy. *J Appl Physiol* 118: 783–793, 2015.
53. **West JB, Milledge JS, Schoene RB.** *High altitude medicine and physiology*. London: Hodder Arnold, 2007.
54. **Wüst RC, McDonald JR, Sun Y, Ferguson BS, Rogatzki MJ, Spires J, Kowalchuk JM, Gladden LB, Rossiter HB.** Slowed muscle oxygen uptake kinetics with raised metabolism are not dependent on blood flow or recruitment dynamics. *J Physiol* 592: 1857–1871, 2014.
55. **Wüst RC, Myers DS, Stones R, Benoist D, Robinson PA, Boyle JP, Peers C, White E, Rossiter HB.** Regional skeletal muscle remodeling, and mitochondrial dysfunction in right ventricular heart failure. *Am J Physiol Heart Circ Physiol* 302: H402–H411, 2012.